



Removal of magnesium and calcium from electric furnace titanium slag by H_3PO_4 oxidation roasting–leaching process

Fu-qiang ZHENG¹, Yu-feng GUO¹, Shui-shi LIU^{1,2}, Guan-zhou QIU¹, Feng CHEN¹, Tao JIANG¹, Shuai WANG¹

1. School of Minerals Processing and Bioengineering, Central South University, Changsha 410083, China;

2. Zhongye Changtian International Engineering Co., Ltd., Changsha 410083, China

Received 30 November 2016; accepted 28 March 2017

Abstract: H_3PO_4 oxidation roasting followed by HCl acid leaching was proposed to remove magnesium and calcium from electric furnace titanium slag containing 3.12% MgO and 0.86% CaO. XRF, XRD and SEM techniques were used to characterize the composition, mineral phase component and microstructure of the titanium slag. The H_3PO_4 oxidation thermodynamic, mineral phase transformation, microstructure, element distribution in titanium slag during H_3PO_4 oxidation process and leaching process were investigated. The thermodynamic analysis indicated that H_3PO_4 could promote the decomposition of $MgTi_2O_5$ and $CaSiO_3$. The results indicated that H_3PO_4 could effectively promote the transformation of titanium-bearing mineral to rutile and enrich the impurities in $M_xTi_{3-x}O_5$ into phosphate which could be removed by acid leaching process. Under the studied conditions, the leaching rates of magnesium and calcium reached 94.68% and 87.19%, respectively. The acid leached slag containing 0.19% MgO and 0.13% CaO (mass fraction) was obtained.

Key words: titanium slag; oxidation roasting; leaching; H_3PO_4 ; magnesium; calcium; rutile

1 Introduction

TiO_2 pigment is widely used in industries due to its superior performance [1–3]. Currently, the chloride process and sulfate process have been two main commercial processes for TiO_2 pigment production [4]. The development of sulfate process is restricted by the low-quality TiO_2 pigment and environment problem. Compared with sulfate process, the chloride process has received more attention due to the advantages of high-quality TiO_2 pigment and smaller amount of waste [5]. In the chloride process, Cl_2 chlorinates the upgraded titanium slag/rutile to produce $TiCl_4$ in the presence of carbon. The major impurities in feedstock, such as Mg and Ca, are also chlorinated to form metal chlorides in the carbochlorination process. However, $CaCl_2$ and $MgCl_2$ are so non-volatile under the conditions of chlorination reaction that these chlorides will clog the reaction bed [6]. Therefore, the strict (CaO + MgO) content (less than 1.5%, mass fraction) of feedstock in the chloride process is proposed to prevent the reaction bed from being clogged by $CaCl_2$ and $MgCl_2$.

With the decrease of natural rutile supply, more and

more attention is paid to preparing the high-quality titanium slag or synthetic rutile for the feedstock of chloride process. There are many methods developed or under development all over the world to prepare the high-quality titanium slag or synthetic rutile from ilmenite, including the electric furnace smelting process [7], the Becher process [8], the acid leaching [9] and other methods [10,11]. The electric furnace smelting process has been commercialized due to the advantages of large production scale, low waste and high efficiency, while the other methods are still immature due to the technological problems. Panxi region of China is rich in ilmenite containing high (CaO + MgO) content, which accounts for 16.8% titanium of world reserve [12]. Currently, the electric furnace titanium slag produced in smelting process using Panzhihua ilmenite cannot meet the quality requirement of chloride feedstock because of its low TiO_2 content and high (CaO + MgO) content. Thus, it is crucial to develop an effective method to remove the impurities of electric furnace titanium slag, especially magnesium and calcium.

There are many studies on removing the impurities and upgrading the electric furnace titanium slag [13–15]. The common processes are oxidation/reduction of

titanium slag followed by leaching to remove the impurities. The UGS process [16] is a typical method for upgrading sored slag to synthetic rutile containing 94% TiO₂ and 0.6% (CaO + MgO) in Canada. LEDDY and SCHECHTER [17] indicated that the TiO₂ content of the titanium slag increased from 70% to 90% (mass fraction) by oxidation roasting–leaching process, and the (CaO + MgO) content in the final product was less than 0.2%. ELGER and HOLMES [18] proposed that the titanium slag was roasted in the SO₂/SO₃ and O₂ atmospheres at 600–1000 °C. Then, the roasted slag was leached by water to prepare the synthetic rutile which contains 85.5% TiO₂, 0.07% CaO and 1.3% MgO (mass fraction). The titanium slag reacted with sodium hydroxide in order to transform to the soluble titanate which could be washed and separated from the insoluble impurities [19]. Then, titanate was further treated to obtain the final product with the high TiO₂ content (>99%). LASHEEN [20] and DONG et al [21] pointed out that the titanium slag was roasted with sodium salt to break the structure, then the roasted slag could be upgraded to the synthetic rutile by water leaching or acid leaching. NAYL et al [5] pointed out that titanium slag could dissolve in the NH₄OH system at 150 °C, then the ammonium titanate was hydrolyzed to obtain the high purity titanium dioxide. The improvement of this process was proposed by SUI and ZHAI [22], during which ammonium bisulfate was used to roast with titanium slag. Except the UGS process, the methods mentioned above are still immature due to the technological problems, such as heavy consumers of additive and energy, severe equipment requirements and pollution problems. The UGS process is not suitable for upgrading the Panzhihua titanium slag due to the high (CaO + MgO) content in the slag [23]. How to effectively remove magnesium and calcium from Panzhihua titanium slag has become a significant problem, which is crucial for the utilization of Panzhihua titanium slag and the development of titanium industry in China.

In this work, the removal of magnesium and calcium from Panzhihua titanium slag by H₃PO₄ oxidation roasting–leaching was investigated, with an emphasis on H₃PO₄ oxidation thermodynamic, the effects of H₃PO₄ dosage and reaction temperature on the mineral phase transformation, microstructure and element distribution of roasted slag, and the effects of H₃PO₄ dosage on the leaching rates of magnesium and calcium. We proposed an effective method of removing magnesium and calcium from Panzhihua titanium slag.

2 Experimental

2.1 Materials

The titanium slag used in this study was collected

from The Titanium Slag Plant of Panzhihua Iron & Steel Company, Sichuan Province, China. The samples were finely ground to size less than 74 μm. The chemical composition of the Panzhihua titanium slag is listed in Table 1. It can be seen that the TiO₂, MgO and CaO contents of the titanium slag are 72.43%, 3.12% and 0.86% (mass fraction), respectively. The XRD pattern and microstructure of Panzhihua titanium slag are shown in Fig. 1 and Fig. 2, respectively. The EDS analysis of the titanium slag is listed in Table 2. The major titanium-bearing mineral in the slag is M_xTi_{3-x}O₅ (0 < x < 2, M=Ti, Fe, Mg, Al). Most of the magnesium exists in the titanium-bearing mineral. All reagents used in the

Table 1 Chemical composition of Panzhihua titanium slag (mass fraction, %)

TiO ₂	TFe	Al ₂ O ₃	SiO ₂	CaO	MgO	MnO	P ₂ O ₅
72.43	9.26	2.55	7.39	0.86	3.12	0.83	0.013

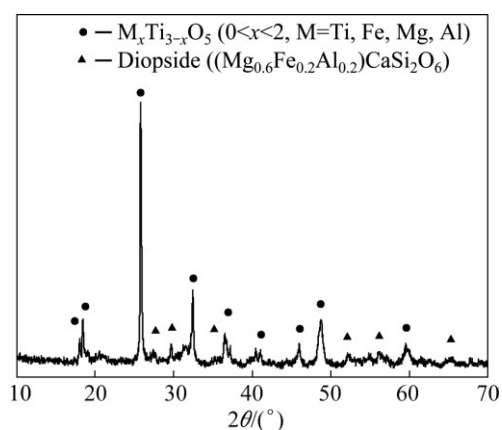


Fig. 1 XRD pattern of Panzhihua titanium slag

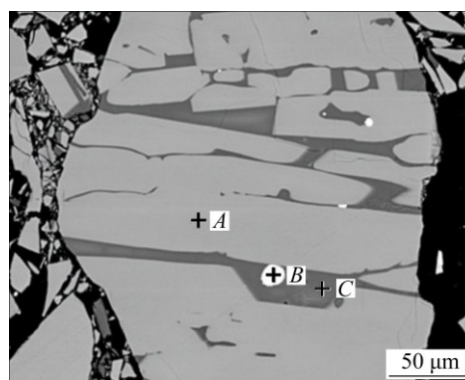


Fig. 2 SEM image of Panzhihua titanium slag

Table 2 EDS analysis of titanium slag

Point in Fig. 2	Mass fraction/%							
	O	Ti	Fe	Mg	Ca	Al	Si	S
A	26.62	61.43	5.98	3.53	–	1.39	–	–
B	–	2.28	60.54	–	–	–	–	37.18
C	46.03	3.78	3.12	2.41	15.43	4.23	24.81	–

experiments are at least of analytical grade. The purity of oxygen is 99.99%.

2.2 Experimental procedure

2.2.1 Roasting

Before roasting, 100 g titanium slag was thoroughly blended with a certain amount of 85% H_3PO_4 . Then, the mixture was pelletized into green pellets (2 g per pellet) with 10 mm in diameter. The green pellets were dried in an oven at 110 °C for 4 h. Roasting experiments were carried out in a horizontal tube resistance furnace (diameter 50 mm) with an automatic temperature control system. 20 g dried pellets were loaded in a corundum crucible (10 mm × 25 mm × 55 mm) which was pushed into the furnace at a rate of 25 mm/min. Then, the pellets were heated at designated temperatures for a certain time with the oxygen flow through horizontal tube at a rate of 0.3 L/min. After roasting, the oxygen was closed and the corundum crucible was pulled out of the furnace at a rate of 25 mm/min. Then, the oxidized samples were cooled to room temperature and submitted for the analysis of mineral phase, microstructure, element distribution and the leaching experiment.

2.2.2 Leaching

The oxidized pellets were crushed and ground to size less than 74 μm firstly. HCl leaching experiments were carried out in a 500 mL three-necked glass flask fitted with a thermometer, an agitator at a stirring rate of 500 r/min and a reflux condenser. The three-necked glass flask was heated in a constant temperature oil-bathing. 100 g leaching agent (20% HCl, mass fraction) was loaded into the flask and heated to the designated temperature. Then, 20 g oxidized sample was put into the leaching agent. After leaching, the slurry was filtered and washed with distilled water. The filter cake was dried in an oven at 105 °C for 4 h. The dried acid leached slag was submitted for the analysis of chemical composition and mineral phase.

2.3 Definition of parameters

The leaching rate of impurities is calculated by using Eq. (1):

$$\eta_i = \left(1 - \frac{mw_i}{m_0w_0} \right) \times 100\% \quad (1)$$

where η_i (%) is the leaching rate of impurities, m (g) is the mass of the dried leaching residue, w_i (%) is the mass fraction of impurity in the leached residue, m_0 (g) is the mass of oxidized titanium slag used in the leaching experiment, and w_0 (%) is the mass fraction of impurity in the oxidized titanium slag.

2.4 Analysis and characterization

FactSage 7.0 (Thermfact/CRCT, Montreal, QC, Canada; GTT-Technologies, Herzogenrath, Germany) was used to analyze the thermodynamics.

The chemical compositions of the titanium slag, oxidized sample and leached sample were quantitatively analyzed by X-ray fluorescence (XRF, Axios mAX, Holand PANalytical Co., Ltd.).

The microstructure and the element distribution of the mineral in the samples were characterized by a scanning electron microscope equipped with an energy diffraction spectrum analyzer (SEM-EDS, Quanta200, FEI, Holland).

The phase compositions of the samples were characterized by X-ray diffractometry (Cu K_α radiation, $\lambda=0.154056$ nm, 40 kV, 300 mA, D/max2550PC, Rigaku Co., Ltd., Japan).

3 Results and discussion

3.1 Thermodynamic analysis of roasting

In order to make the thermodynamic calculation, the $M_xTi_{3-x}O_5$ can be simply considered as Ti_3O_5 , $FeTi_2O_5$, $MgTi_2O_5$ and Al_2TiO_5 . The possible reactions of titanium-bearing minerals during the oxidation roasting can be simply expressed in Table 3.

Figure 3 shows the $\Delta G^\ominus-T$ relationship lines of the possible reactions during oxidation roasting. According to the calculated results, all the ΔG^\ominus values of Eqs. (2)–(6) increase with the increase of oxidation temperature. The ΔG^\ominus of Eq. (6) is above the zero line. This indicates that $MgTi_2O_5$ cannot be decomposed into MgO and TiO_2 , which is detrimental to the further acid leaching process. The ΔG^\ominus values of Eqs. (4) and (5) are above zero at 1139.37 and 1532.29 K, respectively.

The silicate in the titanium slag can be simply considered as $CaSiO_3$ which may react with H_3PO_4 . The possible reactions during the H_3PO_4 oxidation roasting

Table 3 Possible chemical reactions of titanium-bearing minerals during oxidation roasting

Equation No.	Reaction	$\Delta G^\ominus-T$ relationship
(2)	$2Ti_3O_5 + O_2 = 6TiO_2$	$\Delta G^\ominus = -767547.97 + 225.72T$
(3)	$4FeTi_2O_5 + O_2 = 2Fe_2TiO_5 + 6TiO_2$	$\Delta G^\ominus = -532794.55 + 258.20T$
(4)	$Fe_2TiO_5 = Fe_2O_3 + TiO_2$	$\Delta G^\ominus = -23619.15 + 20.73T$
(5)	$Al_2TiO_5 = Al_2O_3 + TiO_2$	$\Delta G^\ominus = -44375.19 + 28.96T$
(6)	$MgTi_2O_5 = MgO + 2TiO_2$	$\Delta G^\ominus = 12871.86 + 10.85T$

process can be simply expressed in Table 4. The $\Delta G^\ominus-T$ relationship lines of the possible reactions during H_3PO_4 oxidation roasting are shown in Fig. 4.

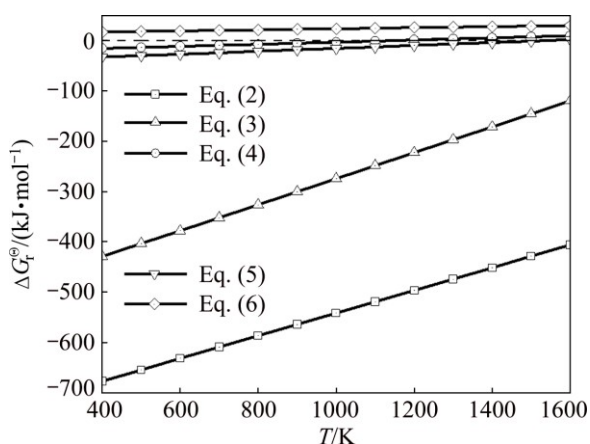


Fig. 3 $\Delta G^\ominus-T$ relationship lines of possible reactions during oxidation roasting

Table 4 Possible chemical reactions during H_3PO_4 oxidation roasting

Equation No.	Reaction	$\Delta G^\ominus-T$ relationship
(7)	$2H_3PO_4 = P_2O_5 + 3H_2O$	$\Delta G^\ominus = 483468.8 - 298.5T$
(8)	$Fe_2TiO_5 + 2H_3PO_4 = 2FePO_4 + TiO_2 + 3H_2O$	$\Delta G^\ominus = -424415 + 334.09T$
(9)	$3MgTi_2O_5 + 2H_3PO_4 = Mg_3(PO_4)_2 + 6TiO_2 + 3H_2O$	$\Delta G^\ominus = -173041 - 211.5T$
(10)	$Al_2TiO_5 + 2H_3PO_4 = 2AlPO_4 + TiO_2 + 3H_2O$	$\Delta G^\ominus = -31132 - 261.9T$
(11)	$3CaSiO_3 + 2H_3PO_4 = Ca_3(PO_4)_2 + 3SiO_2 + 3H_2O$	$\Delta G^\ominus = -209529 - 230T$

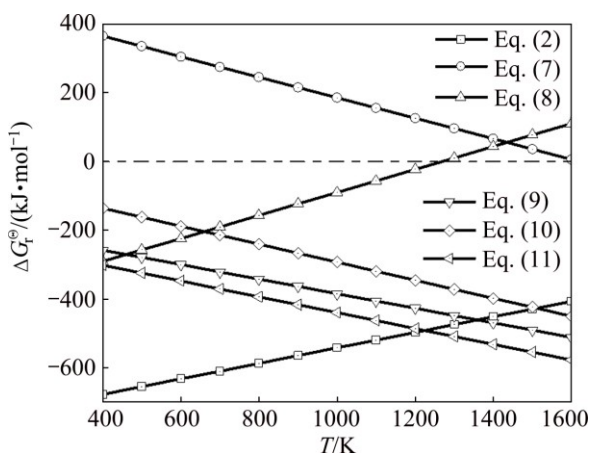


Fig. 4 $\Delta G^\ominus-T$ relationship lines of possible reactions during H_3PO_4 oxidation roasting

The ΔG^\ominus value of Eq. (7) is above the zero line, which indicates that H_3PO_4 cannot be decomposed in the temperature range of 400–1600 K. Except Eq. (8), the

ΔG^\ominus values of other reactions are less than zero, which means that adding H_3PO_4 in the titanium slag is advantageous to the removal of Ca and Mg in the temperature range of 400–1600 K. Therefore, the titanium-bearing minerals and $CaSiO_3$ in the titanium slag can react with H_3PO_4 to generate the phosphates during H_3PO_4 oxidation roasting.

3.2 Comparison of oxidation roasting and H_3PO_4 oxidation roasting

Figure 5 shows the XRD patterns of different roasted slags at 1200 °C for 120 min. The H_3PO_4 dosage is 16% (mass fraction) during the H_3PO_4 oxidation roasting. The rutile phase is detected in the oxidized slag and H_3PO_4 oxidized slag. The intensity of rutile phase in the H_3PO_4 oxidized slag is much higher than that of the oxidized slag. The intensity of $M_xTi_{3-x}O_5$ ($0 < x < 2$) becomes very weak in the H_3PO_4 oxidized slag.

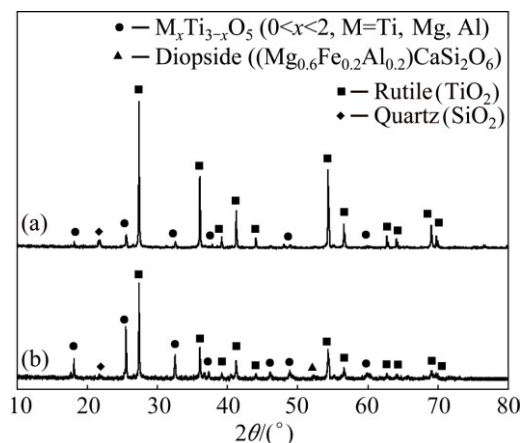


Fig. 5 XRD patterns of different roasted slags: (a) H_3PO_4 oxidized slag; (b) Oxidized slag

The SEM images and EDS analysis of the two oxidized slags are shown in Fig. 6 and Table 5, respectively. It is observed from Fig. 6(a) and Table 5 that the long columnar rutile particle with about 4 μm in width is embedded in $M_xTi_{3-x}O_5$ ($0 < x < 2$) particle. The analysis of Point A2 in Fig. 6(a) indicates that a large amount of Ti coexists with Al, Mg and Fe in the $M_xTi_{3-x}O_5$ ($0 < x < 2$) particle. It can be seen from Fig. 6(b) that the 10–30 μm granular rutile particles connect with each other in the H_3PO_4 oxidized slag. The phosphates (Points B4 and B5) are formed during H_3PO_4 oxidation roasting.

The impurities leaching rates of different slags are shown in Fig. 7. The leaching conditions are as follows: HCl acid concentration 20%, leaching temperature 110 °C, leaching time 120 min and liquid/solid ratio 5:1. This indicates that the impurities leaching rates are improved effectively by the H_3PO_4 oxidation roasting, especially for magnesium.

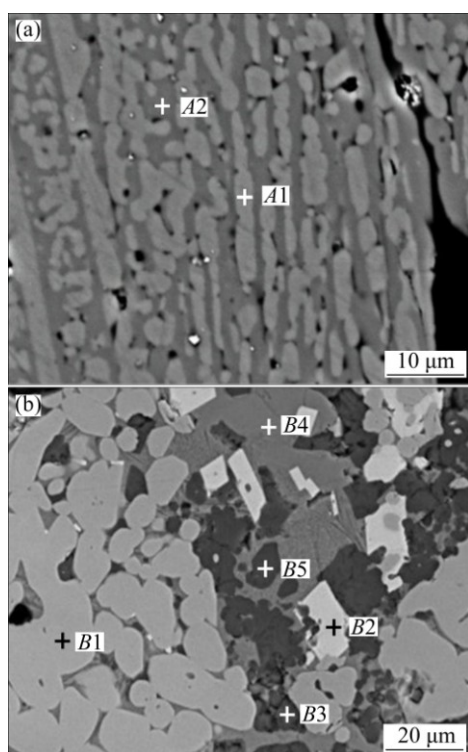


Fig. 6 SEM images of different titanium slags: (a) Oxidized slag roasted at 1200 °C for 120 min; (b) H₃PO₄ oxidized slag roasted at 1200 °C for 120 min with 16% H₃PO₄

Table 5 EDS analysis of different titanium slags

Point in Fig. 6	Mass fraction/%							
	O	Ti	Fe	Mg	Ca	Al	Si	P
A1	38.71	61.29	–	–	–	–	–	–
A2	14.83	50.22	22.60	7.06	–	2.90	–	–
B1	51.10	48.90	–	–	–	–	–	–
B2	40.02	22.59	35.07	1.06	0.15	1.07	0.04	–
B3	58.18	1.27	–	0.26	–	–	39.49	0.81
B4	49.89	2.61	7.17	10.10	5.37	3.63	0.37	20.88
B5	56.35	0.52	2.54	–	0.07	16.31	1.74	22.48

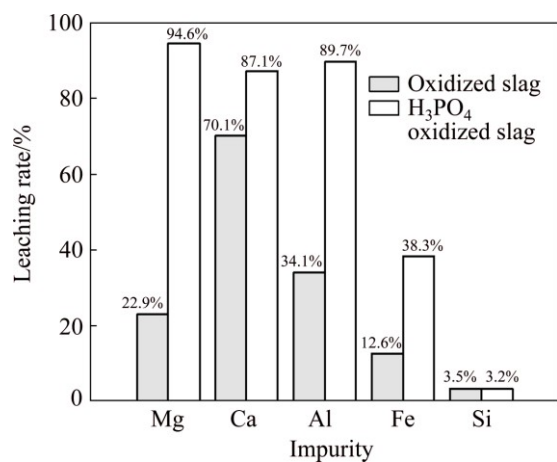


Fig. 7 Impurities leaching rates of different slags

Therefore, the transformation of rutile is enhanced by H₃PO₄ oxidation roasting. In the H₃PO₄ oxidation roasting, the impurities are transformed to phosphates which can be removed by the HCl leaching. Under the same oxidation conditions, the magnesium leaching rate of H₃PO₄ oxidized slag reaches 94.6%, which is much higher than that of oxidized slag (22.9%).

3.3 Oxidation roasting

3.3.1 Effect of H₃PO₄ dosage on oxidation roasting

The effect of H₃PO₄ dosage on the phase composition of H₃PO₄ oxidized slag at 1000 °C for 120 min is shown in Fig. 8. The results indicate that the intensity of rutile increases and the intensity of M_xTi_{3-x}O₅ (0 < x < 2) decreases with the increase of H₃PO₄ dosage. When the H₃PO₄ dosage reaches 12% (mass fraction), the peak of quartz is detected in the H₃PO₄ oxidized slag, which indicates that a large amount of silicate reacts with H₃PO₄. When the H₃PO₄ dosage is 20% (mass fraction), the intensity of M_xTi_{3-x}O₅ (0 < x < 2) becomes very weak and the major mineral phase of the H₃PO₄ oxidized slag is rutile. The phosphorus-bearing minerals are not detected in different H₃PO₄ oxidized slags, because the phosphate produced in the roasting process may be non-crystalline substance which cannot be detected by XRD analysis.

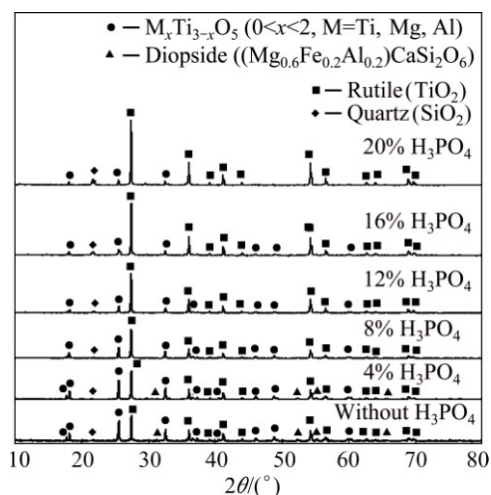


Fig. 8 XRD patterns of roasted slags with different H₃PO₄ dosages at 1000 °C for 120 min

Figure 9 and Table 6 show SEM images and EDS analysis of H₃PO₄ oxidized slag with different H₃PO₄ dosages at 1000 °C for 120 min. It can be seen from Fig. 9 and Table 6 that many small holes appear at the edge of roasted particle as the H₃PO₄ dosage is 4%. And the EDS analyses (Points B1 and B2 in Fig. 9(b)) indicate that the main impurities still distribute in M_xTi_{3-x}O₅ (0 < x < 2) and silicate. When the H₃PO₄ dosage is 8%, the particle edge is broken and many long cracks stretch into the particles.

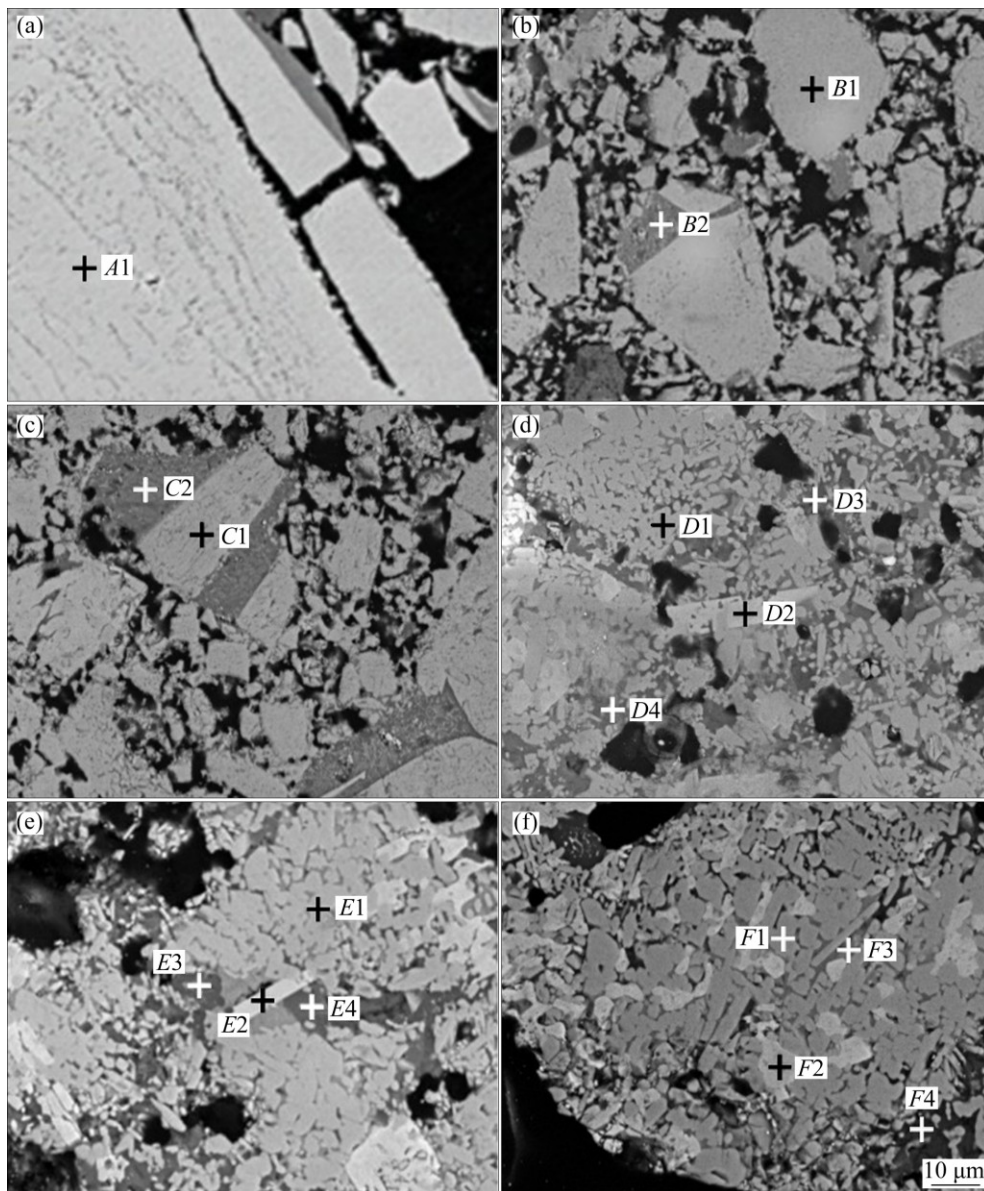
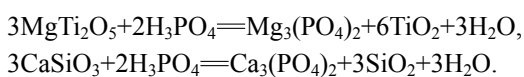


Fig. 9 SEM images of roasted titanium slag with different H_3PO_4 dosages at $1000\text{ }^\circ\text{C}$ for 120 min: (a) Without H_3PO_4 ; (b) 4% H_3PO_4 ; (c) 8% H_3PO_4 ; (d) 12% H_3PO_4 ; (e) 16% H_3PO_4 ; (f) 20% H_3PO_4

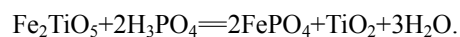
The EDS analyses (Points C1 and C2 in Fig. 9(c)) show that the main impurities still distribute in $\text{M}_x\text{Ti}_{3-x}\text{O}_5$ ($0 < x < 2$) and silicate.

When the H_3PO_4 dosage reaches 12%, the titanium slag particle is broken into small parts. According to the EDS analysis in Table 6 and the XRD analysis in Fig. 8, the gray part (Point D1 in Fig. 9(d)) is rutile, and the gray-white part (Point D2 in Fig. 9(d)) is pseudobrookite. In addition, Point D3 in Fig. 9(d) is SiO_2 and Point D4 in Fig. 9(d) is $\text{Mg}_3(\text{PO}_4)_2$. The results are consistent with the thermodynamic analysis in Fig. 4. Therefore, when the H_3PO_4 dosage reaches 12%, the main reactions during the roasting are as follows:



$\text{Ca}_3(\text{PO}_4)_2$ is not detected in the SEM images because of the less content in the slag.

When the H_3PO_4 dosage increases to 16%, the rutile particles are larger than those of 12% H_3PO_4 oxidized slag. The gray part (Point E1 in Fig. 9(e)) is rutile. The gray-white part (Point E2 in Fig. 9(e)) is pseudobrookite, which is clear-enrichment in the roasted slag. Point E3 in Fig. 9(e) is SiO_2 . The main chemical compositions of Point E4 in Fig. 9(e) are O, P, Mg and Fe, which indicates that Fe_2TiO_5 starts to react with H_3PO_4 as follows:



It is observed from the EDS analysis in Table 6 that the main mineral phases in 20% H_3PO_4 roasted slag are similar to that of 16% H_3PO_4 oxidized slag. The rutile

Table 6 EDS analysis of roasted titanium slag with different H₃PO₄ dosages

Mass fraction of H ₃ PO ₄ / %	Point in Fig. 9	Mass fraction/%							
		O	Ti	Fe	Mg	Ca	Al	Si	P
0	A1	15.73	62.19	11.41	7.06	–	3.61	–	–
4	B1	50.23	41.87	4.80	1.32	0.10	1.17	0.12	0.38
	B2	55.17	6.16	1.60	2.78	8.74	4.34	20.51	–
8	C1	54.07	36.99	3.27	2.97	0.24	1.42	0.29	0.74
	C2	52.41	3.68	5.58	3.46	5.75	4.63	24.08	–
12	D1	46.73	53.27	–	–	–	–	–	–
	D2	44.61	24.29	28.98	1.35	–	0.76	–	–
	D3	58.48	1.29	–	–	–	0.51	39.61	0.12
	D4	58.30	–	–	20.05	–	–	–	19.93
16	E1	48.00	52.00	–	–	–	–	–	–
	E2	44.63	23.79	29.85	0.90	–	0.83	–	–
	E3	60.56	3.42	–	–	–	0.39	35.05	0.58
	E4	51.44	–	1.57	21.64	–	–	–	21.68
20	F1	49.93	50.07	–	–	–	–	–	–
	F2	44.29	20.14	33.24	1.05	–	0.22	0.24	0.81
	F3	60.88	5.79	0.43	0.37	–	0.92	29.81	1.81
	F4	51.70	–	4.30	18.88	–	–	–	22.47

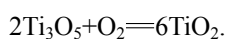
particles are much larger than those of 16% H₃PO₄ oxidized slag. The phosphates migrate to the edge of titanium slag particle.

When the H₃PO₄ dosage is less than 12%, the impurities in slag cannot be observably separated from titanium-bearing mineral. When the H₃PO₄ dosage is 16%, the iron in the slag starts to react with H₃PO₄ to form phosphate. In addition, the rutile, pseudobrookite, quartz and phosphate observably are enriched in the slag. Therefore, in order to transform more impurities into phosphates, the H₃PO₄ dosage should be at least 16%.

3.3.2 Effect of reaction temperature on oxidation roasting

The effect of reaction temperature on the phase composition of H₃PO₄ oxidized slag is shown in Fig. 10. During the H₃PO₄ oxidation roasting, H₃PO₄ dosage is 16% and the reaction time is 120 min.

Based on the results in Fig. 10, increasing the temperature can promote mineral phase transformation during the H₃PO₄ oxidation roasting. When the reaction temperature is 600 °C, the main mineral phases are similar to those of untreated titanium slag, which indicates that the reactions between H₃PO₄ and titanium slag do not occur or occur very slowly. When the reaction temperature reaches 800 °C, the intensity of M_xTi_{3-x}O₅ (0<x<2) is weakened and the rutile phase is detected. Then, the main reaction at 800 °C during H₃PO₄ oxidation roasting is as follows:



When the reaction temperature increases to 1000 °C,

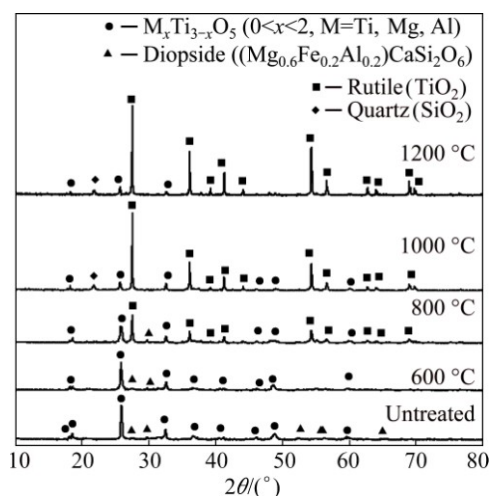


Fig. 10 XRD patterns of roasted slags at different reaction temperatures for 120 min with 16% H₃PO₄

the rutile is the main mineral phase in the H₃PO₄ oxidized slag. The intensity of M_xTi_{3-x}O₅ (0<x<2) is weakened sharply, which means a large amount of M_xTi_{3-x}O₅ (0<x<2) reacts with H₃PO₄. The disappearance of silicate peak and the appearance of quartz peak indicate that the silicate reacts with H₃PO₄.

When the reaction temperature reaches 1200 °C, the main mineral phases in slag are similar to those of H₃PO₄ oxidized slag at 1000 °C. The intensity of rutile is higher than that of H₃PO₄ oxidized slag at 1000 °C.

Figure 11 and Table 7 show SEM images and EDS analysis of H₃PO₄ oxidized slags with 16% H₃PO₄ at

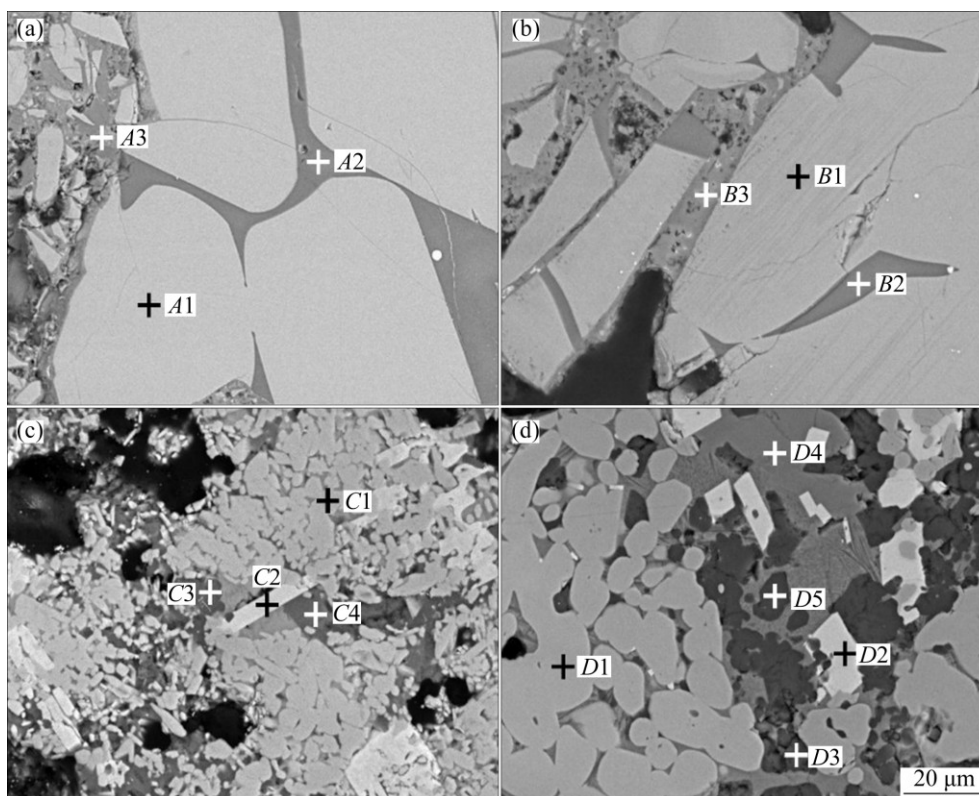


Fig. 11 SEM images of roasted titanium slag at different reaction temperatures for 120 min with 16% H_3PO_4 : (a) 600 °C; (b) 800 °C; (c) 1000 °C; (d) 1200 °C

Table 7 EDS analysis of roasted titanium slag at different reaction temperatures

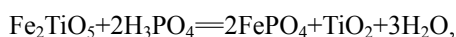
Temperature/ °C	Point in Fig. 11	Mass fraction/%							
		O	Ti	Fe	Mg	Ca	Al	Si	P
600	A1	43.41	50.33	4.03	1.34	–	0.94	0.04	–
	A2	64.36	2.44	0.64	1.37	5.82	4.21	20.77	–
	A3	53.31	6.01	4.21	1.02	4.08	3.00	17.35	11.01
800	B1	42.92	46.08	8.56	1.65	–	0.79	–	–
	B2	54.54	5.88	–	1.12	5.48	5.37	27.61	–
	B3	52.53	4.40	1.97	3.35	4.32	3.07	18.34	12.03
1000	C1	48.00	52.00	–	–	–	–	–	–
	C2	44.63	23.79	29.85	0.90	–	0.83	–	–
	C3	60.56	3.42	–	–	–	0.39	35.05	0.58
	C4	51.44	–	1.57	21.64	–	–	–	21.68
1200	D1	51.10	48.90	–	–	–	–	–	–
	D2	40.02	22.59	35.07	1.06	0.15	1.07	0.04	–
	D3	58.18	1.27	–	0.26	–	–	39.49	0.81
	D4	49.89	2.61	7.17	10.10	5.37	3.63	0.37	20.88
	D5	56.35	–	2.54	–	0.07	16.31	1.74	22.48

different reaction temperatures for 120 min, respectively. As shown in Fig. 11 and Table 7, when the reaction temperatures are 600 and 800 °C, the microstructures and mineral compositions of the roasted slag have no obvious changes. The P and Si distribute around the

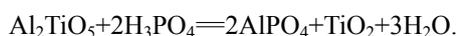
$M_xTi_{3-x}O_5$ ($0 < x < 2$) particles (Points A3 and B3 in Figs. 11(a) and (b), respectively). And the main chemical compositions of $M_xTi_{3-x}O_5$ ($0 < x < 2$) (Points A1 and B1 in Figs. 11(a) and (b), respectively) and silicate (Points A2 and B2 in Figs. 11(a) and (b), respectively) almost do not

change. The rutile is not detected in the SEM image due to its tiny crystal although it is detected in the XRD pattern of H_3PO_4 oxidized slag at $800\text{ }^\circ\text{C}$.

When the reaction temperature reaches $1000\text{ }^\circ\text{C}$, the titanium slag particle is broken into small parts. At the same time, the H_3PO_4 reacts with $\text{M}_x\text{Ti}_{3-x}\text{O}_5$ ($0 < x < 2$) and silicate sufficiently. The main mineral phases in the roasted slag are rutile (Point C1 in Fig. 11(c)), pseudobrookite (Point C2 in Fig. 11(c)), quartz (Point C3 in Fig. 11(c)) and phosphate (Point C4 in Fig. 11(c)). When the reaction temperature is $1000\text{ }^\circ\text{C}$, the main reactions during H_3PO_4 oxidation roasting are as follows:



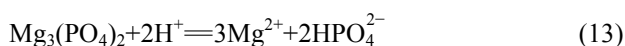
When the reaction temperature is $1200\text{ }^\circ\text{C}$, the sizes of different minerals are much larger than those of H_3PO_4 oxidized slag at $1000\text{ }^\circ\text{C}$. There are two kinds of phosphates in the H_3PO_4 oxidized slag. One is magnesium-rich phosphate (Point D4 in Fig. 11(d)) and the other is aluminum-rich phosphate (Point D5 in Fig. 11(d)). This indicates that when the reaction temperature is $1200\text{ }^\circ\text{C}$, Al_2TiO_5 reacts with H_3PO_4 as follows:



Therefore, increasing reaction temperature can effectively promote the transformation of impurities in the slag into phosphates, especially magnesium and aluminum.

3.4 Effect of H_3PO_4 dosages on HCl leaching

The titanium slags are oxidized with different dosages of H_3PO_4 at $1000\text{ }^\circ\text{C}$ for 120 min. The impurities in the slag react with H_3PO_4 to form orthophosphate such as $\text{Mg}_3(\text{PO}_4)_2$ and $\text{Ca}_3(\text{PO}_4)_2$ at the high oxidation temperature. The H_3PO_4 oxidized slag is leached by hydrochloric acid under the following leaching conditions: hydrochloric acid concentration 20%, leaching temperature $110\text{ }^\circ\text{C}$, leaching time 120 min, liquid/solid ratio 5:1. The phosphate in the H_3PO_4 oxidized slag can be removed by hydrochloric acid leaching. Because the molar ratio of $\text{HCl}/(\text{CaO}+\text{MgO})$ is less than 18:1, the leaching products will be $\text{Mg}(\text{H}_2\text{PO}_4)_2$ and $\text{Ca}(\text{H}_2\text{PO}_4)_2$, or MgHPO_4 and CaHPO_4 , which can be dissolved in hydrochloric acid [24]. Therefore, the leaching mechanisms are as follows:



The effects of H_3PO_4 dosage on the Mg and Ca leaching rates and the TiO_2 content of acid leached slag are shown in Fig. 12. The leaching rates of Mg and Ca increase with the increase of H_3PO_4 dosage. When the H_3PO_4 dosage is 16%, the leaching rates of Mg and Ca reach 94.68% and 87.19%, respectively. The H_3PO_4 dosage has a significant influence on the TiO_2 content of acid leached slag. The TiO_2 content of acid leached slag reaches 81.84% from 73.85% (mass fraction) as H_3PO_4 dosage increases from 0 to 20%. Table 8 shows the chemical composition of acid leached slag when H_3PO_4 dosage is 16%. It is seen from Table 8 that the MgO and CaO contents of acid leached slag are 0.19% and 0.13% (mass fraction), respectively. The XRD patterns of different acid leached slags under the same oxidation conditions ($1000\text{ }^\circ\text{C}$, 120 min) are shown in Fig. 13. The

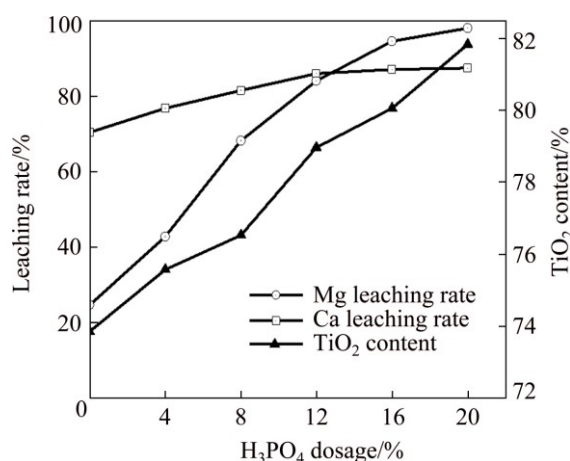


Fig. 12 Effect of H_3PO_4 dosage on Mg and Ca leaching rates and TiO_2 content of acid leached slag

Table 8 Chemical composition of hydrochloric acid leaching product (mass fraction, %)

TiO_2	TFe	Al_2O_3	CaO	MgO	SiO_2	P_2O_5
80.06	6.79	0.31	0.13	0.19	7.44	2.83

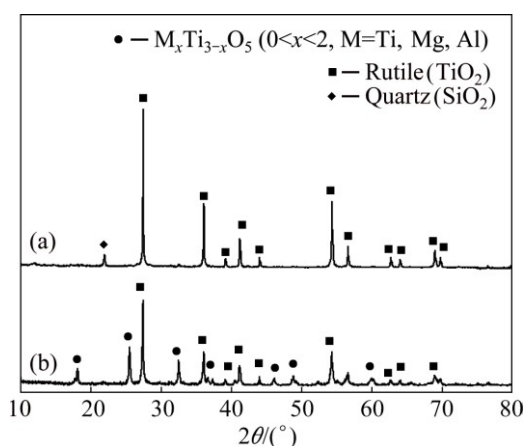


Fig. 13 XRD patterns of different acid leaching products: (a) H_3PO_4 oxidized-leached slag; (b) Oxidized-leached slag

results in Fig. 13 indicate that the major mineral phases of H_3PO_4 oxidized-leached slag are rutile and quartz. The $M_xTi_{3-x}O_5$ was not detected in the H_3PO_4 oxidized-leached slag.

4 Conclusions

1) H_3PO_4 oxidation roasting followed by acid leaching was proposed to remove magnesium and calcium from electric furnace titanium slag containing 3.12% MgO and 0.86% CaO.

2) The oxidation thermodynamics of titanium-bearing minerals during the oxidation roasting process indicated that H_3PO_4 could promote the decomposition of $MgTi_2O_5$ and $CaSiO_3$.

3) The transformation of titanium slag into rutile and Mg leaching rate effectively increased with the increase of H_3PO_4 dosage and reaction temperature.

4) After the titanium slag was oxidized with 16% H_3PO_4 at 1000 °C for 120 min, most of Mg and Ca in the H_3PO_4 oxidized slag could be removed by HCl leaching. The magnesium and calcium leaching rates reached 94.68% and 87.19%, respectively. A product containing 0.19% MgO and 0.13% CaO was obtained.

References

- [1] QIAO Li-ying, XIE Feng-yu, XIE Ming-hui, GONG Cai-hua, WANG Wei-lang, GAO Jia-cheng. Characterization and photo-electrochemical performance of Zn-doped TiO_2 films by sol-gel method [J]. Transactions of Nonferrous Metals Society of China, 2016, 26(8): 2109–2116.
- [2] DANISH R, AHMED F, ARSHI N, ANWAR M S, KOO B H. Facile synthesis of single-crystalline rutile TiO_2 nano-rods by solution method [J]. Transactions of Nonferrous Metals Society of China, 2014, 24(S1): s152–s156.
- [3] PAN Yin-cheng, ZOU Jian-xin, ZENG Xiao-qin, DING Wen-jiang. Hydrogen storage properties of Mg– TiO_2 composite powder prepared by arc plasma method [J]. Transactions of Nonferrous Metals Society of China, 2014, 24(12): 3834–3839.
- [4] CROCE P S, MOUSAVI A. A sustainable sulfate process to produce TiO_2 pigments [J]. Environmental Chemistry Letters, 2013, 11(4): 325–328.
- [5] NAYL A A, ISMAIL I M, ALY H F. Ammonium hydroxide decomposition of ilmenite slag [J]. Hydrometallurgy, 2009, 98(1–2): 196–200.
- [6] XU Cong, YUAN Zhang-fu, WANG Xiao-qiang. Preparation of $TiCl_4$ with the titanium slag containing magnesia and calcia in a combined fluidized bed [J]. Chinese J Chem Eng, 2006, 14(3): 281–288.
- [7] SAHU K K, ALEX T C, MISHRA D, AGRAWAL A. An overview on the production of pigment grade titania from titania-rich slag [J]. Waste Management & Research, 2006, 24(1): 74–79.
- [8] BALDERSON G F, MACDONALD C A. Method for the production of synthetic rutile: US patent, 5885324 [P]. 1999–03–23.
- [9] EL-HAZEK N, LASHEEN T A, EL-SHEIKH R, ZAKI S A. Hydrometallurgical criteria for TiO_2 leaching from Rosetta ilmenite by hydrochloric acid [J]. Hydrometallurgy, 2007, 87(1–2): 45–50.
- [10] WU Ling, LI Xin-hai, WANG Zhi-xing, WANG Xiao-juan, LI Ling-jun, FANG Jie, WU Fei-xiang, GUO Hua-jun. Preparation of synthetic rutile and metal-doped $LiFePO_4$ from ilmenite [J]. Powder Technology, 2010, 199(3): 293–297.
- [11] LI Zeng-he, WANG Zhen-cui, LI Ge. Preparation of nano-titanium dioxide from ilmenite using sulfuric acid-decomposition by liquid phase method [J]. Powder Technology, 2016, 287: 256–263.
- [12] ZHENG Fu-qiang, CHEN Feng, GUO Yu-feng, JIANG Tao, YAKOVLEVICH T A, QIU Guan-zhou. Kinetics of hydrochloric acid leaching of titanium from titanium-bearing electric furnace slag [J]. JOM, 2016, 68(5): 1476–1484.
- [13] ZHANG Li, LI Guang-qiang, ZHANG Wu. Synthesis of rutile from high titania slag by pyrometallurgical route [J]. Transactions of Nonferrous Metals Society of China, 2011, 21(10): 2317–2322.
- [14] SUI Li-li, ZHAI Yu-chun. Reaction kinetics of roasting high-titanium slag with concentrated sulfuric acid [J]. Transactions of Nonferrous Metals Society of China, 2014, 24(3): 848–853.
- [15] CHEN Guo, CHEN Jin, PENG Jin-hui, WAN Run-dong. Green evaluation of microwave-assisted leaching process of high titanium slag on life cycle assessment [J]. Transactions of Nonferrous Metals Society of China, 2010, 20(S1): s198–s204.
- [16] GUÉGUIN M, CARDARELLI F. Chemistry and mineralogy of titania-rich slags. Part 1: Hemo-ilmenite, sulphate, and upgraded titania slags [J]. Mineral Processing and Extractive Metallurgy Review, 2007, 28(1): 1–58.
- [17] LEDDY J J, SCHECHTER D L. Pressure leaching of titaniferous material: US patent, 3060002A [P]. 1962–05–20.
- [18] ELGER G W, HOLMES R A. Purifying titanium-bearing slag by promoted sulfation: US patent, 4362557 [P]. 1982–12–07.
- [19] WANG Dong, CHU Jing-long, LI Jie, QI Tao, WANG Wei-jing. Anti-caking in the production of titanium dioxide using low-grade titanium slag via the NaOH molten salt method [J]. Powder Technology, 2012, 232: 99–105.
- [20] LASHEEN T A. Soda ash roasting of titania slag product from Rosetta ilmenite [J]. Hydrometallurgy, 2008, 93(3–4): 124–128.
- [21] DONG Hai-gang, JIANG Tao, GUO Yu-feng, CHEN Jia-lin, FAN Xing-xiang. Upgrading a Ti-slag by a roast-leach process [J]. Hydrometallurgy, 2012, 113–114: 119–121.
- [22] SUI Li-li, ZHAI Yu-chun. Extraction of TiO_2 from high titanium slag through roasting by ammonium bisulfate [J]. The Chinese Journal of Nonferrous Metals, 2014, 24(3): 826–830. (in Chinese)
- [23] ZHANG Jian-bo, LIAO Jun-hui, CHENG Xiao-zhe, YE Si-dong. Contrastive study on processes of redox modification-acid leaching of Panzhihua Ti-slag and ilmenite [J]. Chinese Journal of Rare Metals, 2016, 40(4): 385–392. (in Chinese)
- [24] DEMIRBAS A, ABALI Y, MERT E. Recovery of phosphate from calcinated bone by dissolution in hydrochloric acid solutions [J]. Resour Conserv Recy, 1999, 26(3–4): 251–258.

电炉钛渣磷酸化焙烧—浸出脱除镁、钙杂质

郑富强¹, 郭宇峰¹, 刘水石^{1,2}, 邱冠周¹, 陈凤¹, 姜涛¹, 王帅¹

1. 中南大学 资源加工与生物工程学院, 长沙 410083;

2. 中冶长天国际工程有限责任公司, 长沙 410083

摘 要: 提出一种利用磷酸化焙烧—盐酸浸出从电炉钛渣(含 3.12% MgO 和 0.86% CaO)中有效脱除镁、钙杂质的方法。利用 XRF、XRD 和 SEM 对钛渣样品的化学成分、物相成分和显微组织进行表征。研究钛渣的磷酸氧化焙烧热力学、氧化焙烧过程中钛渣物相的转变、显微组织和元素分布的变化以及浸出除杂过程。热力学分析结果表明, 焙烧过程中加入磷酸能有效促进 MgTi_2O_5 和 CaSiO_3 的分解。研究结果表明, 在焙烧过程中磷酸能有效促进渣中含钛矿物转变为金红石, 并促使 $\text{M}_x\text{Ti}_{3-x}\text{O}_5$ 中杂质元素富集在磷酸盐中, 进而通过酸浸除去。在所研究的实验条件下, 钛渣中镁和钙的脱除率可分别达到 94.68%和 87.19%。最终酸浸渣中 MgO 和 CaO 含量可分别降低至 0.19%和 0.13%(质量分数)。

关键词: 钛渣; 氧化焙烧; 浸出; 磷酸; 镁; 钙; 金红石;

(Edited by Wei-ping CHEN)